Stress-resultant based elasto-plastic analysis for a concrete plate

Jinsang Chung[1] and Nam H. Kim[2]

Department of Mechanical and Aerospace Engineering
University of Florida, Gainesville, FL 32611, USA

Abstract

In this paper, a stress-resultant based elasto-plastic model for a concrete plate is presented as a substitute of a layered model, which is commonly used and requires many sub-layers in order to describe a nonlinear stress distribution over the thickness. Iliushin's failure function is extended to a concrete plate based on the Drucker-Prager yield criterion after a modification from a parametric study. Two new parameters are introduced to the yield function in order to describe the non-symmetric, fully plastic moment of a concrete plate and the coupled behavior of membrane and bending actions. General plastic rules are applied to the stress-resultant based yield criterion. In addition, an integrated section method using equivalent material coefficients is presented for the stress-resultant based concrete plate for steel rebar reinforcement. Several numerical test models are compared with the layered model for the purposed of verification.

Keywords: Stress-resultant model, Concrete plate, Elasto-plastic plate, Integrated section method.

1. Introduction

According to the development of CAD/CAE technology, nowadays, many structural engineers want to simulate their structures as it stands without any simplification, and thus, the modeling of a building or civil structure become more detail and sometime requires several tens of thousands of elements. Therefore, a huge amount of numerical calculation is required to obtain a reasonably accurate resistance for a structure against various internal and external loadings. Currently developed numerous computer systems and numerical methods make it possible to conduct such a large amount of calculation.

Generally, civil structures are designed to be elastic to maintain structural integrity under ordinary and predictable loading scenarios. Sometimes, however, simulations beyond the elastic limit are also required to estimate collapse patterns and weak points under unexpected loading, such as earthquake.

[1] Graduate student, jschung@ufl.edu
[2] Corresponding author, Associate Professor, nkim@ufl.edu, Tel)1-352-575-0665, Fax) 1-352-392-7303

Finding weak points can be useful for an evenly distributed collapse mode, which creates a safe structure in severe conditions. Numerical simulations beyond the elastic limit require much more calculation.

The nonlinear material behavior of plates and beams can be described in different ways, as illustrated in Figure 1. Since traditional failure criteria of materials are defined using local stress-strain relations, the solid model in Figure 1(a) is the most ideal for the simulations beyond the elastic limit, but with the expense of the most computational resources. The failure state can be estimated in each solid, layer, or section, depending on whether the solid, layered or section models are used. When it comes to a real multi-story building or a multi-span bridge under earthquake loadings, the solid model is nearly impossible due to a huge amount of numerical calculations involved; elasto-plastic stress-strain relation must be calculated at every integration point. Therefore, computationally more efficient nonlinear simulation methods are required to reduce the simulation cost. For that purpose, the layered model is commonly used for a plate element, and the fiber or resultant section models are used for a frame element [8, 13]. However, the layered model and the fiber section model also require lots of numerical calculation and information storage because integration needs to be performed at each layer and fiber. To apply the nonlinear analysis to a large structure, more efficient methods are required, and thus, the stress-resultant based methods are develped in this paper.

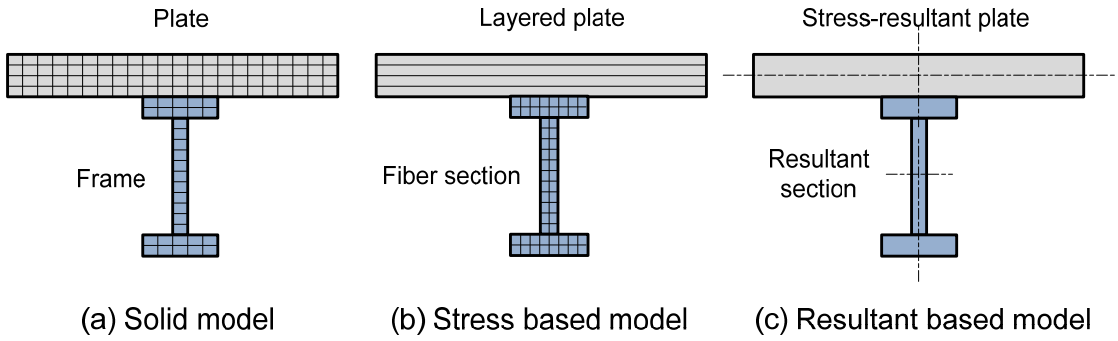

Figure 1: Modeling methods for nonlinear simulation of a structural member.

A frame element has been a major objective for modeling a nonlinear behavior by many researchers due to the fact that lots of types of structures can be modeled by the frame element. Sectional material nonlinearity of a frame element is considered by two different models: the resultant section model and the fiber section model. The resultant section model which defines the sectional nonlinear response using moment-curvature relations has been presented by Takeda et al. [3], Hilmy and Adel [4], Hajjar and Gourley [5] and El-Tawil and Deierlein [7]. The fiber section model estimates the response of section based on the uni-axial stress-strain relation of each fiber cell consisting a frame section. The uni-axial

constitutive model of concrete has been presented by Kent and Park [9], Mander et al. [10] and El-Tawil and Deierlein [6].

In plate elements, material nonlinearity can be simulated by either the layered model or the stress-resultant based model. In general, the layered model can be used for any type of failure criteria because it is based on the local stress-strain relation. On the other hand, the stress-resultant based model has mainly been applied to metal plates based on von-Mises criterion. Firstly, the yield function based on stress-resultants was suggested by Iliushin [11], and it has been modified to describe the Bauschinger effect by Bieniek and Funaro [17]. The progressive development of plastic zone under bending moment was described by a plastic curvature parameter suggested by Crisfield [12]. The influence of transverse shear forces on the plastic behavior was incorporated into the stress-resultant yield function by Shi and Voyiadjis [13]. An extension from a frame yield criterion to the reinforced concrete plate was presented by Koechlin et al. [15]. However, since the yielding moment is a function of membrane forces in combined loadings, it is limited to be used in general applications. Most research on stress-resultant based elasto-plastic behavior is so far focused on a metal plate. In this paper, the stress-resultant based model for a concrete plate is presented. An appropriate yield function is proposed based on theoretical and parametric studies, and general plasticity rules are applied to the yield function. In addition, steel reinforcement is modeled as an integrated section method using equivalent material coefficients.

This paper is organized as follows. Section 2 describes the stress-resultant model for a concrete plate where a yield function using stress-resultants based on the Drucker-Prager failure criterion is presented. Plastic behaviors such as flow rule and plastic consistency parameter are also derived for the proposed yield function. Section 3 explains a steel rebar model which is combined with the stress-resultant model for concrete reinforcement. Section 4 shows numerical comparisons between the proposed model and the layered model with a unit element and a bridge structure, followed by conclusions and discussions in Section 5.

2. Elasto-plastic analysis of a plate element

In this section, an efficient elasto-plastic model based on the stress resultants for a concrete plate is introduced. Generally, for the elasto-plastic behavior of a plate, the layered model is used to take into account the nonlinear stress distribution through the thickness [13]. Stresses at each layer are calculated based on the strains that are assumed linearly distributed. The yield criterion for the elasto-plastic behavior is applied to calculate stresses and tangent stiffness at each layer, which are integrated over the thickness to calculate internal forces and stiffness of the element. The concept of layered model is

described in Figure 2(a), where the constitutive relation between element stresses and strains of a single layer can be written as

$$\Delta\boldsymbol{\sigma} = \mathbf{C} : \left(\Delta\boldsymbol{\varepsilon} - \Delta\boldsymbol{\varepsilon}^{p}\right); \begin{Bmatrix} \Delta\sigma_x \\ \Delta\sigma_y \\ \Delta\sigma_{xy} \end{Bmatrix} = \frac{E}{\left(1-\nu^2\right)} \begin{bmatrix} 1 & \nu & 0 \\ \nu & 1 & 0 \\ 0 & 0 & (1-\nu)/2 \end{bmatrix} \left(\begin{Bmatrix} \Delta\varepsilon_x \\ \Delta\varepsilon_y \\ \Delta\varepsilon_{xy} \end{Bmatrix} - \begin{Bmatrix} \Delta\varepsilon_x{}^{p} \\ \Delta\varepsilon_y{}^{p} \\ \Delta\varepsilon_{xy}{}^{p} \end{Bmatrix} \right) \tag{1}$$

where $\Delta\sigma_{xy}$, $\Delta\varepsilon_{xy}$ and $\Delta\varepsilon_{xy}^{p}$ are incremental stresses, strains and plastic strains, respectively. The subscripts x, y, xy represent the local directions of the components. Once the elasto-plastic stress-strain relationship at each layer is calculated, the relation between stress resultants and the mid-plane strains can be described after integrating over the thickness, as

$$\begin{Bmatrix} \Delta N_x \\ \Delta N_y \\ \Delta N_{xy} \\ \Delta M_x \\ \Delta M_y \\ \Delta M_{xy} \end{Bmatrix} = \begin{bmatrix} A_{11} & A_{12} & A_{16} & B_{11} & B_{12} & B_{16} \\ A_{12} & A_{22} & A_{26} & B_{12} & B_{22} & B_{26} \\ A_{16} & A_{26} & A_{66} & B_{16} & B_{26} & B_{66} \\ B_{11} & B_{12} & B_{16} & D_{11} & D_{12} & D_{16} \\ B_{12} & B_{22} & B_{26} & D_{12} & D_{22} & D_{26} \\ B_{16} & B_{26} & B_{66} & D_{16} & D_{26} & D_{66} \end{bmatrix} \begin{Bmatrix} \Delta\varepsilon_x^{o} \\ \Delta\varepsilon_y^{o} \\ \Delta\varepsilon_{xy}^{o} \\ \Delta\kappa_x \\ \Delta\kappa_y \\ \Delta\kappa_{xy} \end{Bmatrix}, \quad \begin{array}{l} \left(\mathbf{A}_{ij}, \mathbf{B}_{ij}, \mathbf{D}_{ij}\right) = \int_{-h/2}^{h/2} \mathbf{C}_{ij}\left(1, z, z^2\right) dz \quad (i,j = 1,2,6) \\ \Delta\varepsilon_x^{o}, \Delta\varepsilon_y^{o}, \Delta\varepsilon_{xy}^{o} : \text{strains in membrane} \\ \Delta\kappa_x, \Delta\kappa_y, \Delta\kappa_{xy} : \text{curvatures in bending} \\ \Delta N_x, \Delta N_y \Delta N_{xy} : \text{stress resultants for membrane} \\ \Delta M_x, \Delta M_y, \Delta M_{xy} : \text{stress resultatns for bending} \end{array} \tag{2}$$

The accuracy of the above relation depends on the number of layers, which often goes beyond 15. Although reasonable results can be expected in a layered model, a lot of calculation is required because the complicated elasto-plastic behavior should be estimated in every layer at each integration point. In the case of a large structure with tens of thousands of elements, the cost for analysis could be significant.

For efficient calculation of the elasto-plastic behavior of a plate element, the stress-resultant model was proposed, which is based on the Iliushin's yield function [11]. For metals using the von-Mises criterion, a modified yield criterion was suggested by Voyiadjis and Woelke [14]. The concept is described in Figure 2(b), whose yield criterion is explained in the following sub-section. In this model, the yield criterion consists of stress resultants instead of stresses; therefore, no layer-by-layer integration is required. A modified Iliushin's yield function expressed in terms of stress resultants for metal (von-Mises criterion) are applied for the development of plastic deformations across the thickness [14]. In this paper, a modified yield criterion based on Iliushin's yield function for concrete (Drucker-Prager criterion) is proposed for concrete buildings and civil structures. The basic concepts for flow rules are based on the paper of Voyiadjis and Woelke [14].

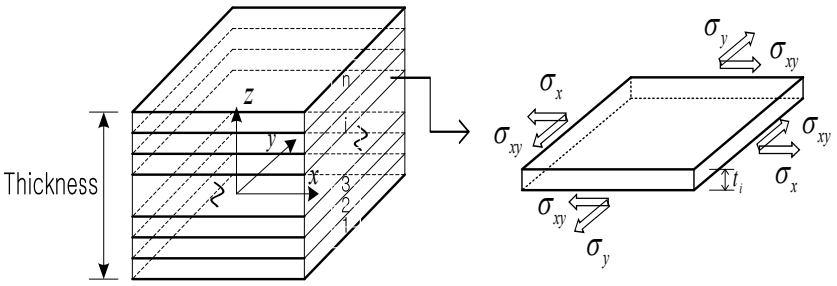

(a) Layered model

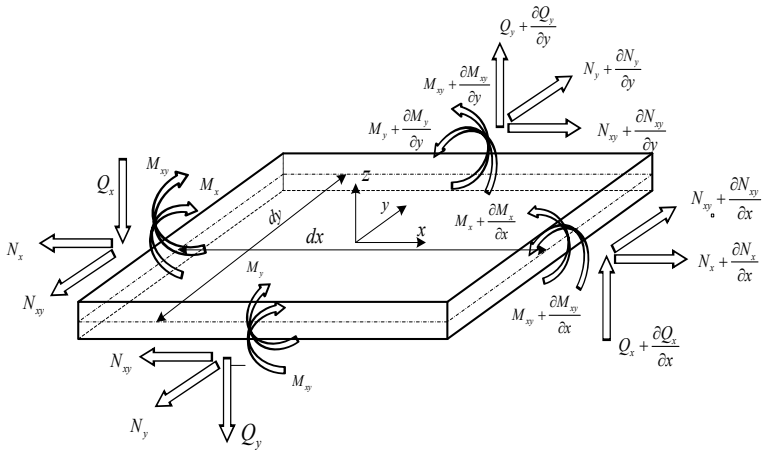

(b) Stress-resultant model

Figure 2 Local coordinate and nonlinear models for elasto-plastic behavior of plate

2.1 Stress resultants based yield function for a concrete plate

For a concrete material, the following form of Drucker-Prager yield criterion is often used:

$$f := A\left(\sigma_{xx} + \sigma_{yy}\right) + \sqrt{\sigma_{xy}^{\,2} - \sigma_{xx}\sigma_{yy} + \frac{1}{3}\left(\sigma_{xx} + \sigma_{yy}\right)^2} - B \le 0 \tag{3}$$

where A and B are material constants, defined as

$$A = \frac{2\sin\phi}{\sqrt{3}\left(3 - \sin\phi\right)}, \quad B = \frac{6c\cos\phi}{\sqrt{3}\left(3 - \sin\phi\right)} \tag{4}$$

where ϕ and c are, respectively, the friction angle and cohesion [2]. For a concrete material, the constant B can be calculated using tensile and compressive yield stresses as $B = \frac{2\sigma_c\sigma_t}{\sqrt{3}\left(\sigma_c + \sigma_t\right)}$. The first term on the right-hand side of Eq. (3) corresponds to the first invariant of stress tensor, and the second term is the second invariant of stress deviator.

The objective is to develop a stress results-based yield criterion from the stress-based criterion in Eq. (3). When a material is in the elastic state, the stresses at the top and bottom of a plate can be expressed in terms of stress resultants as

$$\sigma_{ij} = \frac{N_{ij}}{h} \pm \frac{6M_{ij}}{h^2}, \quad (i, j = 1, 2) \tag{5}$$

where h is the thickness of the plate and N_{ij} and M_{ij} are membrane and moment resultants, respectively. In order to derive the stress resultants based yield criterion, these stresses are substituted into Eq. (3) to yield

$$F = \frac{A}{B_o h}\left(N_{xx} + N_{yy}\right) + \frac{6A}{B_o h^2}\left|M_{xx} + M_{yy}\right| + \frac{1}{\sqrt{3}}\sqrt{\frac{N^2}{\left(B_o h\right)^2} + M^2 \Big/ \left(\frac{B_o h^2}{6}\right)^2 + \frac{12}{B_o{}^2 h^3}\left|NM\right|} - 1 \tag{6}$$

where and B_0 is initial uni-directional yield stress. In the expression of the yield function, the stress resultant intensities, N and M, are given as

$$N^2 = N_{11}^2 + N_{22}^2 - N_{11}N_{22} + 3N_{12}^2 \tag{7}$$

$$M^2 = M_{11}^2 + M_{22}^2 - M_{11}M_{22} + 3M_{12}^2 \tag{8}$$

$$NM = N_{11}M_{11} + N_{22}M_{22} - \frac{1}{2}N_{11}M_{22} - \frac{1}{2}N_{22}M_{11} + 3N_{12}M_{12} \tag{9}$$

Since Eq. (6) is the criterion for the initial yielding, it should be modified for a continuous elasto-plastic behavior of a concrete plate. In the plastic state, the superposition between the membrane and bending actions is not allowed. In addition, the plastic zone starts from the top and bottoms surfaces and gradually move toward inside until the entire cross-section becomes fully plastic. Because of different roles of membrane and bending stress resultants, the moment term of the first invariant of resultants, $\frac{6A}{B_o h^2}\left|M_{xx} + M_{yy}\right|$, is removed due to the fact that this term has both compressive and tensile stresses at the same time even though it comes from the first invariant of stresses, hydrostatic stress. Indeed, this term will show a discrepancy with the reference model in numerical comparison shown in the next section. In addition, the coupled term between membrane and moment components, $\frac{12}{B_o{}^2 h^3}\left|NM\right|$, is also removed through a parametric study and numerical tests. This term was also deleted in the previous research of metal plate based on von-Mises yield criterion for kinematic hardening problem by Armstrong and Frederick [17].

In a concrete plate, the neutral plane deviates from the geometric mid-plane due to plastic deformation. This happens because the tensile yield stress is much less than the compressive one. Three parameters, α, k and β are introduced for progressive plastic deformation, unsymmetric stress distribution and the coupled behavior of membrane and bending resultants. The proposed form of stress-resultants based yield function of a concrete plate can thus be written as

$$F = \frac{A}{N_o}\left(N_{xx} + N_{yy}\right) + \frac{1}{\sqrt{3}}\sqrt{\left(\frac{N}{N_o}\right)^2 + \left(\frac{M^2}{\left(\alpha k M_o\right)^2}\right)^{\beta}} - 1 \tag{10}$$

where N_0 and M_0 are nominal yield membrane and moment resultants of the cross-section, respectively, given as

$$M_o = \frac{B_o h^2}{4}, \quad N_o = B_o h \tag{11}$$

The linear stress expression in Eq. (3) is valid until the initial yield point. Yielding by bending is propagated from the top and bottom planes to the mid-plane as the bending moment increases beyond the initial yielding moment. A specific parameter is required to describe the continuous yielding beyond the initial yielding point. In this paper, followed by Crisfield [12], the plastic curvature parameter α is designed for progressive development of plastic zone under a bending moment as

$$\alpha = 1 - \frac{1}{3.0}\exp\left(-\frac{8}{3}\bar{\kappa}^p\right) \text{ : for matal, } \quad \alpha = 1 - \frac{1}{2.5}\exp\left(-\frac{8}{3}\bar{\kappa}^p\right) \text{ : for concrete} \tag{12}$$

where $\bar{\kappa}^p$ is the equivalent plastic curvature defined by

$$\bar{\kappa}^p = \sum \Delta\bar{\kappa}^p = \frac{Eh}{\sqrt{3}\sigma_o}\sum\left[\left(\Delta\bar{\kappa}_x^p\right)^2 + \left(\Delta\bar{\kappa}_y^p\right)^2 + \left(\Delta\bar{\kappa}_x^p\Delta\bar{\kappa}_y^p\right) + \left(\Delta\bar{\kappa}_{xy}^p\right)^2/4\right]^{\frac{1}{2}} \tag{13}$$

and $\Delta\bar{\kappa}_x^p, \Delta\bar{\kappa}_y^p, \Delta\bar{\kappa}_{xy}^p$ are the incremental plastic curvatures of each direction. The equivalent plastic curvature $\bar{\kappa}^p$ is accumulated value from initial plastic deformation by bending. Therefore, it should be set by zero when it meets an elastic state, which is described in Figure 3. The parameter $\bar{\kappa}^p$ is calculated based on the equivalent plastic curvature.

For a metal plate, the coefficient 1/3 in Eq. (12) is based on symmetric progressive yielding and it is theoretically calculated. The coefficient 1/2.5 in Eq. (12) for concrete is based on unsymmetric yielding of a concrete plate due to the gap between tensile and compressive yielding, and it is numerically estimated by the progressive yielding of a layered concrete plate. For a metal material, yielding is initiated at top and bottom surface at α = 2/3, $\bar{\kappa}^p = 0$, and entire section yielding is occurred at α = 1, $\bar{\kappa}^p = \infty$. For a

concrete plate under bending, initial yielding always occurs at the tensile part and the value of α is 0.6 and $\bar{\kappa}^p = 0$.

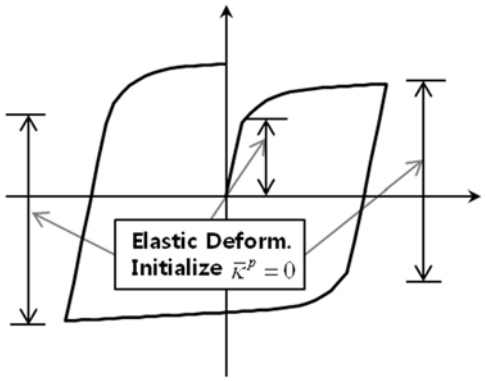

Figure 3 Initializing equivalent plastic curvatures, $\bar{\kappa}^p$

In concrete plates, the stress distribution through the thickness is not symmetric contrary to the metal under elasto-plastic status. The fully plastic moment of a concrete plate cannot be estimated by conventional fully plastic moment, M_o in Eq. (11), due to non-symmetric distribution of stress. In the Drucker-Prager yield criterion, the compressive strength is much larger than the tensile strength, and thus, the neutral axis is shifted to the compressive part. In this paper, parameter k is added to express the fully plastic moment based on M_o in a concrete plate.

In order to derive the parameter k, it is assume that the concrete is in yielding under bending with zero membrane forces. It is also assume that there is no work hardening during plastic deformation. The yield function must satisfy when the material is in the fully plastic state, in which the fully plastic bending moment M_p is applied and the plastic curvature parameter α becomes one. Then, the yield function in Eq. (10) can be expressed as $\frac{1}{\sqrt{3}}\sqrt{\left(M_p^{\,2}\Big/(kM_o)^2\right)^{\beta}} - 1 = 0$ from which the moment calibration parameter, k, is calculated as $k = M_p \Big/ \left(M_o \sqrt{3}^{\,1/\beta}\right)$. The fully plastic moment, M_p, can be calculated by a numerical analysis; for example, the layered model.

In addition to the two parameters, α and k, the yield criterion is further modified in order to match the results with the layered model under combined axial and bending loadings. For that purpose, parameter studies, described in the following section, are conducted and the exponent of the moment term β is introduced.

2.2 Parametric study for a modified yield criterion of a concrete plate

Parametric studies are performed to check the proposed yield function for a concrete plate under combined cases of axial and bending loadings. The parametric studies are executed using pre-axial bending loading and pre-moment axial loading tests. Through comparison between the results of the layered model and those of stress-resultant model, appropriate values of parameters can be found. In this paper, the results from the layered model are considered as a reference. For the purpose of parameter study, the original failure function in Eq. (6) is modified to have three parameters, α, k and β, as

$$F = \frac{A}{B_o h}\left(N_x + N_y\right) + \underbrace{\frac{6A}{B_o h^2}\left|M_x + M_y\right|}_{\text{I1\_M}} + \frac{1}{\sqrt{3}}\sqrt{\frac{N^2}{\left(B_o h\right)^2} + \left(\frac{16M^2}{\left(\alpha k B_o h^2\right)^2}\right)^{\beta} + \underbrace{\frac{12}{B_o{}^2 h^3}\left|NM\right|}_{\text{J2\_NM}}} - 1 \tag{14}$$

As explained in the previous section, the two underlined terms are expected to be removed. The first term (I1_M) is from the first invariant of stress tensor and the second term (J2_NM) is from the second invariant of deviatoric stress tensor. These two terms are tested and compared with the reference results in Figure 4(a) with parameter β = 1.0. When the yield function includes these terms, the yielding moments under pre-axial loading show different patterns compared to the results of the layered model. The I1_M term makes the maximum yielding moment to occur at different pre-axial loadings, while the J2_NM term makes the maximum occurs at zero pre-axial loading. Although the curve without these two terms is still different from the curve form the layered model, it is found that this curve follows the trend correctly. Based on the numerical results with and without I1_M and J2_MN terms in Figure 4(a), these two terms are excluded from the failure function. Now, in order to calibrate the difference in amplitude between the layered model and the proposed failure function, an exponent, β, is introduced for moment term of the second deviatoric stress invariant tensor. In the parameter study of the exponent β in Figure 4(b), it turned out that the value of 0.39 matches well with that of the layered model, which is used for the following analysis. Also, the pre-moment tensile and compressive axial loading cases are investigated in Figure 4(c) and (d). The results of the modified yield function well coincide with those of the layered model when the exponent β is 0.39.

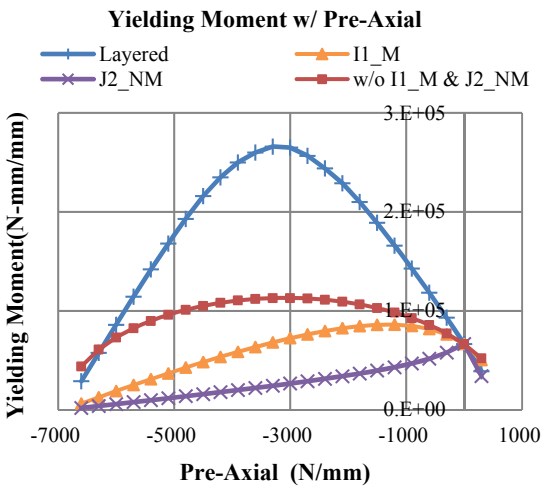

(a) Yielding Moment on Pre-Axial

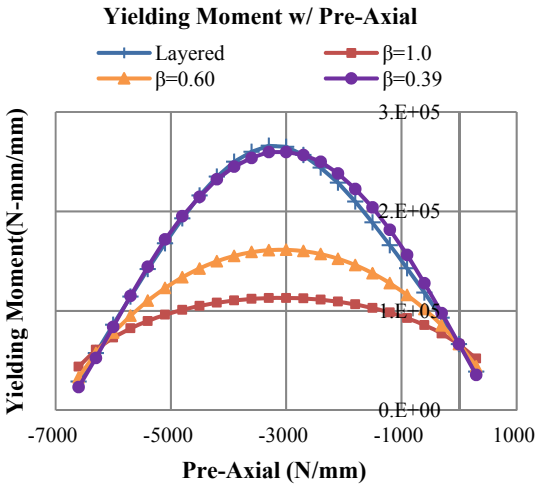

(b) Yielding moment with the exponent β

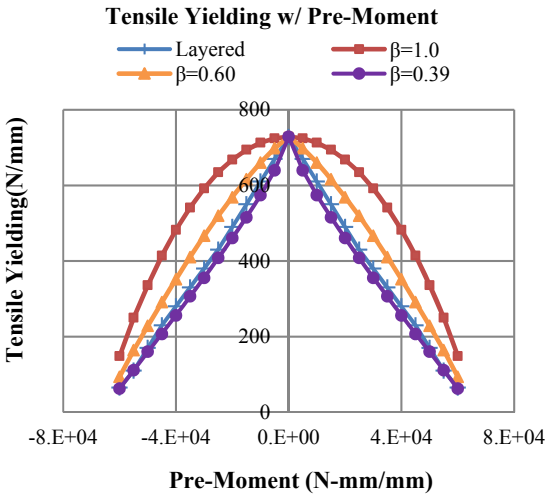

(c) Tensile Yielding on Pre-Moment

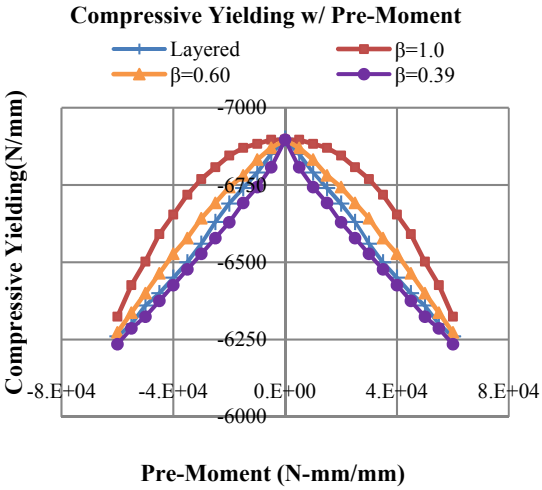

(d) Compressive Yielding on Pre-Moment

Figure 4 Yielding stress resultants in combined loading cases

2.3 General plastic rule

To describe the behavior of elasto-plastic plates, the constitutive law and the flow rule are required. The hypo-elastic constitutive relation is written in the rate form as

$$\dot{\mathbf{s}} = \mathbf{E}\left(\dot{\mathbf{e}} - \dot{\mathbf{e}}^{p}\right) \tag{15}$$

where the rate of stress resultant $\dot{\mathbf{s}}$ and that of strain rate $\dot{\mathbf{e}}$ are defined as

$$\begin{aligned} \dot{\mathbf{s}} &= \left\{ \dot{N}_x \quad \dot{N}_y \quad \dot{N}_{xy} \quad \dot{M}_x \quad \dot{M}_y \quad \dot{M}_{xy} \quad \dot{Q}_x \quad \dot{Q}_y \right\}^T \\ \dot{\mathbf{e}} &= \left\{ \dot{\varepsilon}_x \quad \dot{\varepsilon}_y \quad \dot{\varepsilon}_{xy} \quad \dot{\kappa}_x \quad \dot{\kappa}_y \quad \dot{\kappa}_{xy} \quad \dot{\gamma}_{xz} \quad \dot{\gamma}_{yz} \right\}^T \end{aligned} \tag{16}$$

In addition, in Eq. (15), $\dot{\mathbf{e}}^p$ is the rate of plastic strain, and **E** describes the relation between the stress resultant rate and mid-plane strains rate in a plate as

$$\mathbf{E} = \begin{bmatrix} S & \nu S & & & & & & & \\ \nu S & S & & & & & & & \\ & & \frac{S(1-\nu)}{2} & & & & & & \\ & & & D & \nu D & & & & \\ & & & \nu D & D & & & & \\ & & & & & \frac{D(1-\nu)}{2} & & & \\ & & & & & & T & & \\ & & & & & & & T & \end{bmatrix} \qquad \begin{aligned} S &= \frac{Eh}{\left(1-\nu^2\right)} \\ D &= \frac{Eh^3}{12\left(1-\nu^2\right)} \\ T &= \frac{5}{12}\frac{Eh}{\left(1+\nu\right)} \end{aligned} \tag{17}$$

where E, ν and h are, respectively, the elastic modulus, Poisson's ratio and thickness of a plate. For an elastic response, it is clear that membrane, bending and transverse shear are not related each other.

The elasto-plastic behavior of the stress-resultant model follows a similar formulation with the stress-based flow rule. In the associated flow rule, the mid-plane plastic strain rate is proportional to the gradient of plastic potential, which is identical to the yield function, as

$$\dot{\mathbf{e}}^p = \dot{\lambda}\frac{\partial F}{\partial \mathbf{s}} \tag{18}$$

where $\dot{\lambda}$ is the plastic consistency parameter. Plastic deformation is in the direction normal to the yield surface, and the amount of plastic deformation is decided by the plastic consistency parameter.

In general, the plastic consistency parameter is non-negative, $\dot{\lambda} \geq 0$ **:** positive during plastic deformation and zero for elastic deformation. On the other hand, the yield function is always non-positive: $F < 0$ for the elastic state and $F = 0$ for the plastic state. In optimization, this is called the Kuhn-Tucker condition and can be expressed as

$$\dot{\lambda} \geq 0, \quad F \leq 0, \quad \dot{\lambda}F = 0 \tag{19}$$

The non-positive property of the yield function is regarded as a constraint, and the plastic consistency parameter plays the role of the Lagrange multiplier corresponding to the inequality constraint. The Kuhn-Tucker condition satisfies all possible states of a material. When the state varies, the condition can have three cases.

(a) Elastic loading $\qquad \dot{F} < 0, \ \dot{\lambda} = 0 \ \Rightarrow \ \dot{\lambda}\dot{F} = 0$

(b) Neutral loading $\qquad \dot{F} < 0, \ \dot{\lambda} = 0 \ \Rightarrow \ \dot{\lambda}\dot{F} = 0$

(c) Plastic loading $\dot{F} = 0, \ \dot{\lambda} > 0 \ \Rightarrow \ \dot{\lambda}\dot{F} = 0$

When the stress is on the yield surface, $\dot{\lambda}F = 0$ is equivalent to $\dot{\lambda}\dot{F} = 0$. In elastic and neutral loadings, $\dot{\lambda} = 0$ and there is no plastic deformation. During plastic loading, $\dot{F}$ is zero which means that the yield function remains zero, and the following condition can be obtained:

$$\dot{F}\left(\mathbf{s},\ \varepsilon_{eq}^{p}\right) = \frac{\partial F}{\partial \mathbf{s}} : \dot{\mathbf{s}} + \frac{\partial F}{\partial \varepsilon_{eq}^{p}} \dot{\varepsilon}_{eq}^{p} = 0 \tag{20}$$

where the rate of equivalent plastic strain can be defined as

$$\dot{\varepsilon}_{eq}^{p} = \sqrt{\frac{2}{3}\left(\left(\dot{\varepsilon}_{x}^{p}\right)^{2} + \left(\dot{\varepsilon}_{y}^{p}\right)^{2} + 2\left(\dot{\varepsilon}_{xy}^{p}\right)^{2}\right)} \tag{21}$$

2.4 Newton-Raphson algorithm for the plastic consistency parameter

In numerical analysis, the rate of plastic consistency parameter is converted into an increment by multiplying it with time increment: $\Delta\lambda = \dot{\lambda}\Delta t$. In a similar way, all rates in the previous section can be considered as increments. In the following derivations, an increment will be used instead of rates. When a concrete has no strain hardening, the plastic consistency parameter can be calculated after substituting Eqs. (15) and (18) into Eq. (20), as

$$\frac{\partial F}{\partial \mathbf{s}} : \mathbf{E} : \Delta\mathbf{e} = \Delta\lambda \left(\frac{\partial F^{T}}{\partial \mathbf{s}} : \mathbf{E} : \frac{\partial F}{\partial \mathbf{s}} \right) \tag{22}$$

$$\Delta\lambda = \frac{\dfrac{\partial F^{T}}{\partial \mathbf{s}} : \mathbf{E} : \Delta\boldsymbol{\varepsilon}}{\left(\dfrac{\partial F^{T}}{\partial \mathbf{s}} : \mathbf{E} : \dfrac{\partial F}{\partial \mathbf{s}} \right)} \tag{23}$$

where the components of $\dfrac{\partial F}{\partial \mathbf{s}}$ are listed in the following equation:

$$\frac{\partial F}{\partial N_x}=\frac{A}{N_0}+\frac{1}{C}\frac{1}{N_0^2}\left(2N_x-N_y\right) \qquad \frac{\partial F}{\partial M_{xx}}=\frac{1}{C}\frac{1}{\left(\alpha\kappa M_o\right)^{2\beta}}\beta\left(M^2\right)^{\beta-1}\left(2M_x-M_y\right)$$

$$\frac{\partial F}{\partial N_y}=\frac{A}{N_0}+\frac{1}{C}\frac{1}{N_0^2}\left(2N_y-N_x\right) \qquad \frac{\partial F}{\partial M_{yy}}=\frac{1}{C}\frac{1}{\left(\alpha\kappa M_o\right)^{2\beta}}\beta\left(M^2\right)^{\beta-1}\left(2M_y-M_x\right)$$

$$\frac{\partial F}{\partial N_{xy}}=\frac{1}{C}\frac{1}{N_0^2}6N_{xy} \qquad \frac{\partial F}{\partial M_{xy}}=\frac{1}{C}\frac{1}{\left(\alpha\kappa M_o\right)^{2\beta}}\beta\left(M^2\right)^{\beta-1}6M_{xy}$$

$$\frac{\partial F}{\partial Q_x}=\frac{1}{C}\frac{1}{N_0^2}6Q_x, \qquad \frac{\partial F}{\partial Q_y}=\frac{1}{C}\frac{1}{N_0^2}6Q_y \tag{24}$$

$$C=2\sqrt{3}\sqrt{\frac{N^2}{N_0^2}+\left(\frac{M^2}{\left(\alpha\kappa M_0\right)^2}\right)^{\beta}}$$

From the incremental form of Eq. (15), the incremental stress resultant forces can be calculated using the plastic consistency parameter as

$$\Delta\mathbf{s}=\mathbf{E}:\left(\mathbf{I}-\frac{\frac{\partial F^T}{\partial\mathbf{s}}:\mathbf{D}:\frac{\partial F}{\partial\mathbf{s}}}{\left(\frac{\partial F^T}{\partial\mathbf{s}}:\mathbf{D}:\frac{\partial F}{\partial\mathbf{s}}\right)}\right)\Delta\boldsymbol{\varepsilon} \tag{25}$$

from which the elasto-plastic tangent stiffness can be obtained as

$$\mathbf{E}_{ep}=\mathbf{E}-\frac{\left(\mathbf{E}:\frac{\partial F}{\partial\mathbf{s}}\right)\otimes\left(\frac{\partial F}{\partial\mathbf{s}}:\mathbf{E}\right)}{\left(\frac{\partial F^T}{\partial\mathbf{s}}:\mathbf{E}:\frac{\partial F}{\partial\mathbf{s}}\right)} \tag{26}$$

The procedure to decide the plastic consistency parameter $\Delta\lambda$ is displayed as a flow chart in Figure 5.

Flow chart for $\Delta\lambda$ and stresses and strains at each integration point

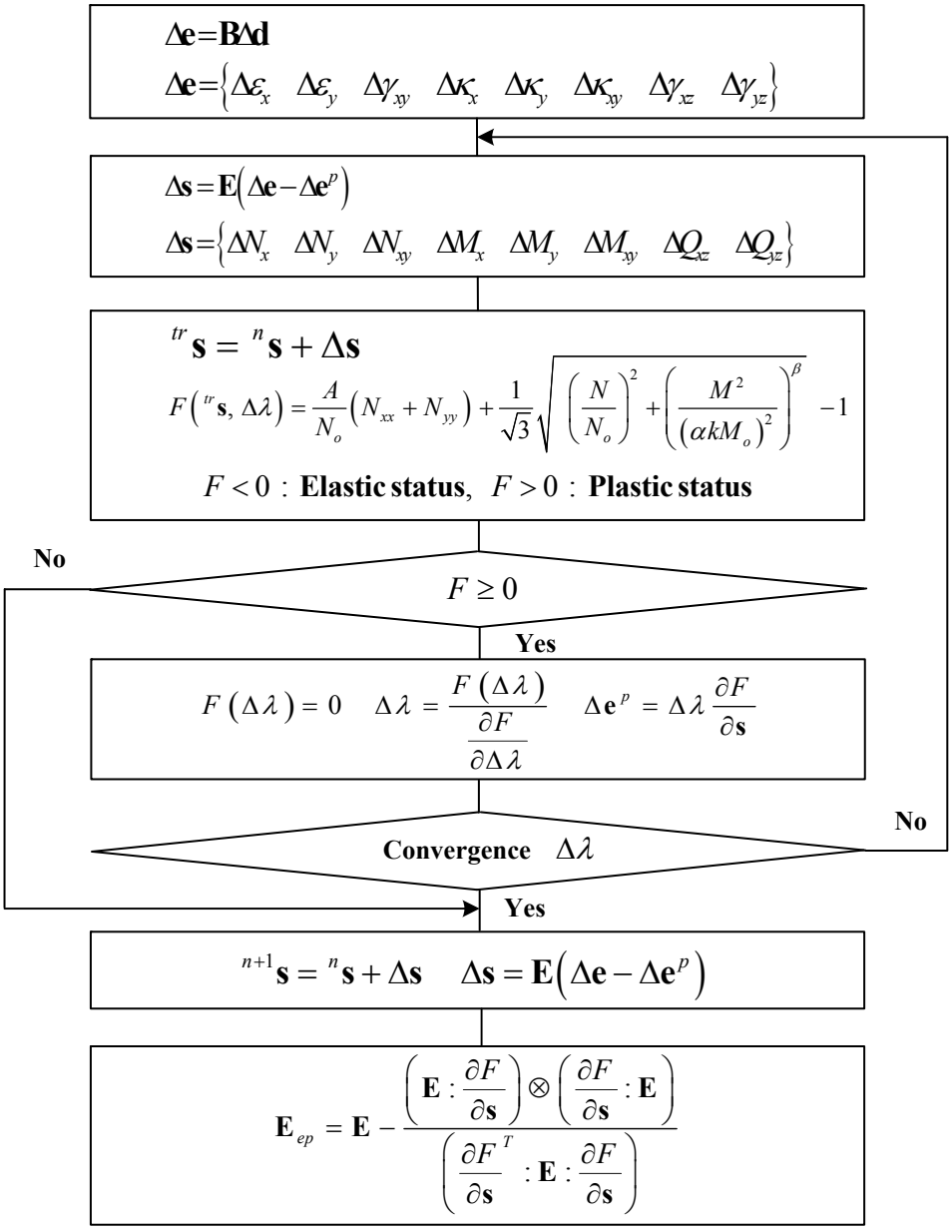

Figure 5 Flow chart for calculating plastic consistency parameter and updating stress resultant

3. Reinforcement of steel rebar

Steel rebar reinforcement is a common way of increasing the strength and ductility of a concrete plate. Since concrete has much less strength in tension than compression, a steel rebar is used for reinforcement of tensile part of concrete. In addition, since concrete is a brittle material, the steel rebar is also used for increasing ductility. Generally, the effect of the steel reinforcement of plate can be considered by two methods. The first is a smeared layer method in which the rebar is assumed as one layer of the plate, and the strains and stresses are calculated with the same way of each concrete ply. The second is an integrated

method in which the effect of rebar is considered by modifying material properties. The smeared method is reasonable for the layered model in which the strain of a rebar can be estimated accurately. The integrated model is applicable to stress-resultant model in which global response is focused rather than individual layer's response.

A general configuration of rebar can be shown in Figure 6(a) with the stress-strain curve in Figure 6(b). There are some assumptions: (i) rigid bond between the rebar and concrete; (ii) linear strain distribution in a section, and (iii) the evenly distributed steel reinforcement in an element. The equivalent thickness of rebar layer is simply calculated using Eq. (27).

$$t_x = A_{xs} \Big/ l_{xs}, \quad t_y = A_{ys} \Big/ l_{ys} \tag{27}$$

where

A_{xs}, A_{ys} : Section area of a x, y direction rebar
l_{xs}, l_{ys} : Space of x, y direction rebar
t_x, t_y : Equivalent thickness of x, y direction rebar

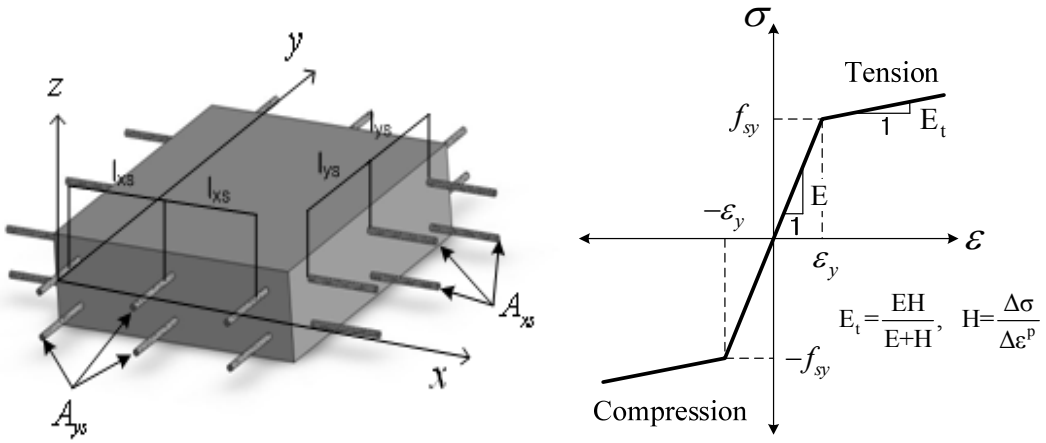

(a) Geometric shape of rebar (b) stress-strain curve of steel rebar

Figure 6 Geometric shape and stress-strain curve of a rebar

3.1 The smeared layer method of rebar reinforcement

A rebar has only one-directional strength and thus the constitutive equation of the rebar layer part can be expressed as Eq. (25). The Eq. (2) can be used for superposition of the results of a rebar layer. In elastic domain, $\bar{E}_x$ and $\bar{E}_y$, the moduli of constitutive equation, are elastic modulus (E) and the tangential modulus (E_t) is used in elasto-plastic domain.

$$\begin{Bmatrix}\Delta\sigma_x\\ \Delta\sigma_y\end{Bmatrix}=\begin{bmatrix}\bar{E}_x & 0\\ 0 & \bar{E}_y\end{bmatrix}\begin{pmatrix}\Delta\varepsilon_x-\Delta\varepsilon_x{}^p\\ \Delta\varepsilon_y-\Delta\varepsilon_y{}^p\end{pmatrix} \tag{28}$$

where $\Delta\sigma_i$, $\Delta\varepsilon_i$ and $\Delta\varepsilon_i{}^p$ are incremental stress, strain and plastic strain vectors respectively.

The yield function of steel rebar can be expressed as Eq. (29) at n step, and at the next step, stress, back stresses and plastic deformation are expressed as Eq. (30). In the elastic range, the stress and back stress can be easily calculated as Eq. (31). In the plastic range, since the yield function should be zero, the incremental plastic deformation and stresses can be calculated as Eq. (32) and the stress, back stress and plastic deformation at n+1 step can be estimated as in Eq. (29). The elasto-plastic tangent modulus is calculated as in Eq. (32).

$$f\left({}^n\sigma,{}^n\alpha,{}^n\varepsilon^p\right)=\left|{}^n\sigma-{}^n\alpha\right|-\left(\sigma_o+\beta_H H\,{}^n\varepsilon^p\right) \tag{29}$$

where ${}^n\sigma$, ${}^n\alpha$, ${}^n\varepsilon^p$ are stress, backstress and plastic strain at n step, and σ_o, H are initial yield stress, plastic modulus respectively.

$$\begin{aligned}{}^{n+1}\sigma &= {}^n\sigma+\Delta\sigma={}^n\sigma+E\left(\Delta\varepsilon-\Delta\varepsilon^p\right)\\ {}^{n+1}\alpha &= {}^n\alpha+\Delta\alpha={}^n\alpha+\left(1-\beta_H\right)H\Delta\varepsilon^p\\ {}^{n+1}\varepsilon^p &= {}^n\varepsilon^p+\Delta\varepsilon^p\end{aligned} \tag{30}$$

Elastic predictor

$$\sigma^{tr}={}^n\sigma+E\Delta\varepsilon,\quad \alpha^{tr}={}^n\alpha,\quad f^{tr}=\left|\sigma^{tr}-\alpha^{tr}\right|-{}^n\sigma_o$$

In elastic range: $f<0$

$${}^{n+1}\sigma=\sigma^{tr}={}^n\sigma+E\Delta\varepsilon,\quad {}^{n+1}\alpha=\alpha^{tr}={}^n\alpha,\quad {}^{n+1}\varepsilon^p={}^n\varepsilon^p \tag{31}$$

In elasto-plastic range: $f\geq 0$

$$f\left({}^{n+1}\sigma,{}^{n+1}\alpha,{}^{n+1}\varepsilon^p\right)=\left|\left({}^n\sigma+E\Delta\varepsilon-{}^n\alpha\right)-\left(\sigma_o+\beta_H H\,{}^n\varepsilon^p\right)\right|-\left(E+H\right)\Delta\varepsilon^p=0 \tag{32}$$

$$\Delta\varepsilon^p=\frac{\left|f^{tr}\right|}{E+H},\quad \Delta\sigma=E\left(1-\frac{f^{tr}}{E+H}\frac{1}{\Delta\varepsilon}\right)\Delta\varepsilon,\quad E_t=\frac{\Delta\sigma}{\Delta\varepsilon}=E\left(1-\frac{f^{tr}}{E+H}\frac{1}{\Delta\varepsilon}\right) \tag{33}$$

3.2 The integrated section method of rebar reinforcement

The rebar reinforcement increases the strength of concrete plate by the strength of itself and the constraint of concrete plate. In elasto-plastic status of a concrete plate, one directional deformation can cause expansional deformation of the orthogonal direction and thus the steel reinforcement gets some tension and the concrete plate has compression at that direction. The constraint of concrete could increase the

strength of yielding. Therefore, the axial yield strength of a reinforced concrete plate is difficult to be estimated using simple analytical equation due to the constraint of rebar reinforcement. In this integrated model, the effect of rebar reinforcement is incorporated with the concrete plate as modified equivalent material coefficients. Since the yield compressive and tensile strength depends on two parameters (A, B) of the Drucker-Prager criterion and material coefficients (c, ϕ) have a relation with the two parameters, the equivalent material coefficients can be estimated based on the axial behavior of a reinforcement concrete plate. In this research, the uni-axial strengths of a reinforced concrete plate are estimated by a numerical analysis using the layered model. The uni-axial tensile and compressive stress resultants of a concrete plate is derived from Eq. (6) and expressed as in Eq. (34) using the two parameters of the Drucker-Prager criterion. The parameters are estimated based on the uni-axial yield stress resultants as in Eq. (35) and the equivalent material coefficient, the cohesion (c) and internal friction angle (ϕ), can be estimated by the relation with the two parameters as in Eq. (36) and Eq. (37).

$$N_o(+) = \frac{\sqrt{3}Bh}{\left(1 + A\sqrt{3}\right)}, \qquad N_o(-) = \frac{\sqrt{3}Bh}{\left(-1 + A\sqrt{3}\right)} \tag{34}$$

$$A = \frac{\left[N_o(-) + N_o(+)\right]}{\sqrt{3}\left[N_o(-) - N_o(+)\right]}, \quad B = \frac{2N_o(+)N_o(-)}{\sqrt{3}h\left[N_o(-) - N_o(+)\right]} \tag{35}$$

$$A = \frac{2\sin\phi}{\sqrt{3}\left(3 - \sin\phi\right)} \Rightarrow \ \phi = \sin^{-1}\frac{3\sqrt{3}A}{\left(2 + \sqrt{3}A\right)} \tag{36}$$

$$B = \frac{6c\cos\phi}{\sqrt{3}\left(3 - \sin\phi\right)} \Rightarrow \ c = \frac{\sqrt{3}B\left(3 - \sin\phi\right)}{6\cos\phi} \tag{37}$$

where $N_o(+)$ and $N_o(-)$ are the tensile and compressive yield strength of a reinforced concrete plate, and A and B are parameters of the Drucker-Prager criterion respectively.

In addition, the elastic modulus is also modified to get the effect of reinforcement as in Eq. (38)

$$E_{eq} = \frac{1}{h}\left(E_c h_c + E_s h_s\right) \tag{38}$$

where E_c and E_s are the elastic modulus of concrete and steel , and h_c and h_s are thickness of concrete and steel parts respectively.

4. Numerical Examples

4.1 Tests of unit element

Results of the stress resultants yield model based on the Drucker-Prager criterion are compared with those of the layered model for a concrete plate nonlinear behavior. Geometry of reinforced concrete plate and

detailed information of reinforced steel rebar are described in Figure 7 and loading conditions are explained in Figure 8. The material coefficients of concrete based on the Drucker-Prager criterion are initial cohesion (c) and initial friction angle (Φ) and both parameters are assumed as c = 4.658 Mpa and Φ = 59.78°. Those coefficients are estimated based on the compressive and tensile yield strengths. The compressive yield strength (f_c) is assumed 34.5 Mpa and the tensile strength (f_t) is estimated by 3.64 Mpa using a formula of ACI-318-08 for a design of concrete floor systems, $f_t = 0.62\sqrt{f_c}$ (Mpa). The area ratio of steel reinforcement is around 1% of concrete section for x and y directions. The elastic modulus of the concrete is assumed as $E = 2.70\times10^4$ Mpa. Generally the concrete does not have strain hardening. Therefore, hardening is not considered in these tests. For the layered model, steel reinforcement is model as a smeared layer and material nonlinearity of rebar is modeled using von-Mises criterion. The elastic modulus and the initial yielding stress of reinforced steel are assumed as $E = 2.10\times10^5$ Mpa and $\sigma_o = 210$ Mpa. For the stress-resultant models, steel reinforcement is considered by the integrated section method using modified material coefficients of concrete. Those values are estimated by Eq. (33) and Eq. (34) and listed in Table 1 according to the area ratio of reinforcement. The hardening effect of reinforced steel is not considered.

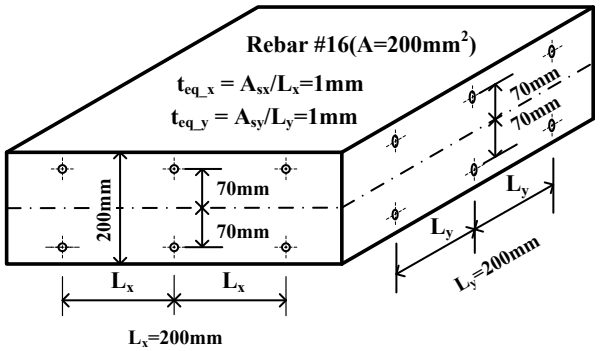

Figure 7 Geometry of a steel reinforced concrete plate

Table 1 Material coefficient for the Drucker-Prager criterion based on integrated method

Rebar reinforcement	No Rebar	0.5% Rebar	0.75% Rebar	1% Rebar
Tensile yield strength (Mpa)	728	960	1070	1175
Compressive yield strength (Mpa)	6900	8540	9350	10160
Cohesion (Mpa)	4.66	5.96	6.58	7.19
Internal friction angle	59.78	58.82	58.54	58.38
Modified elastic modulus (Mpa)	27000	28000	28540	29060

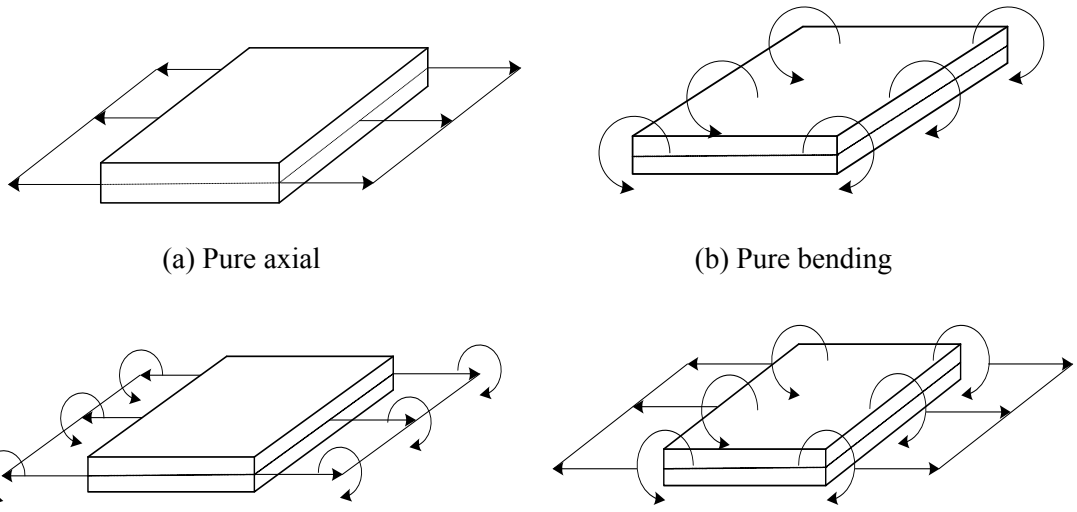

(a) Pure axial (b) Pure bending

(c) Pre-moment axial (d) Pre-axial bending

Figure 8 Test models of stress resultants yield criterion

The results of stress-resultant model based on the Drucker-Prager yield criterion have good agreement with those of the layered model in all unit cases. Those comparisons are shown from Figure 9 to Figure 11. The results of pure axial and pure bending tests under reinforcement show almost same with each other in Figure 9(a) and 9(b). The tensile yield strength of the reinforced concrete plate is around 1170 N/mm which is similar with a simple summation of that of concrete and steel rebar, 1148 N/mm. The compressive yield strength of the plate is around 10160 N/mm which is much larger than a simple summation of that of concrete and steel rebar, 7320 N/mm. The increment of 35% in compressive yield strength is due to the orthogonal direction's confining effect by the rebar.

The comparisons of results of pre-moment axial and pre-axial bending cases are shown in Figure 10 and Figure 11. The Figure 10(a) and 11(a) show the results of without reinforcement and the comparison results under reinforcement are shown in the Figure 10(b) and 11(b). The orthogonal direction confining effect also can be found in bending tests shown in Figure 9(b) in which the bending yield strength is larger around 10%, 106000 N-mm/mm, than a simple summation of concrete and steel strength, 96150 N-mm/mm.

The stress-resultant model under several loading tests shows well matched results compared with the layered model regardless of rebar reinforcement. From these results, the stress-resultant model can be expected to have available accuracy for the material nonlinear behavior of a concrete plate.

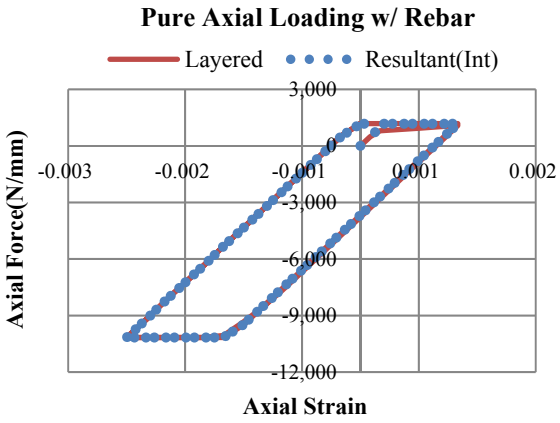

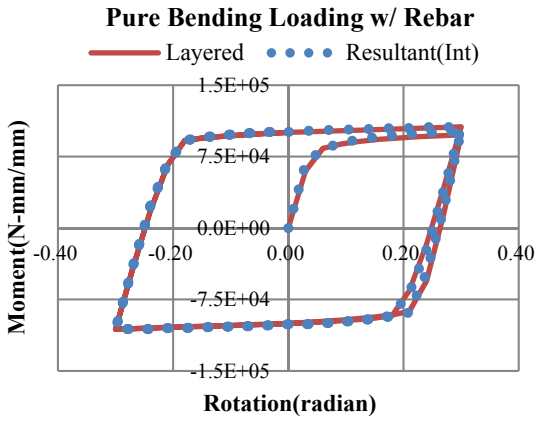

(a) Pure axial loading (b) Pure bending loading

Figure 9 Stress resultants vs. strains in pure loading

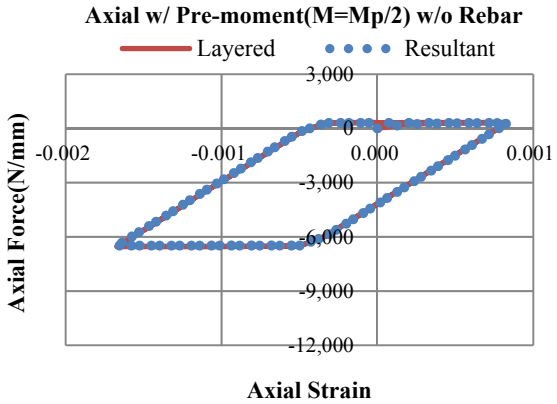

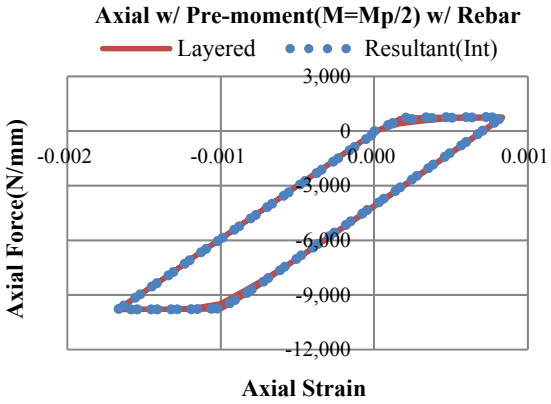

(a) Axial with pre-moment($1/2M_p$) w/o Rebar (b) Axial with pre-moment($1/2M_p$) w/ Rebar

Figure 10 Axial stress resultants vs. strain in pre-moment axial loading

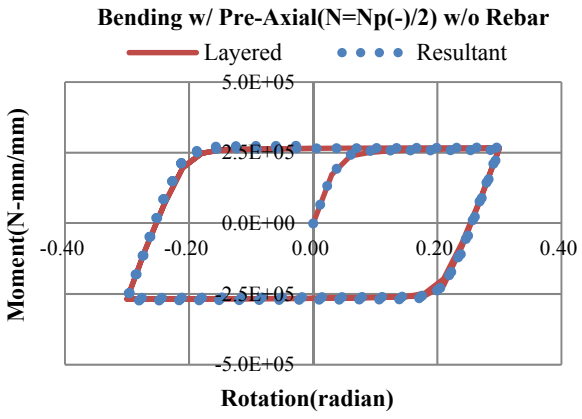

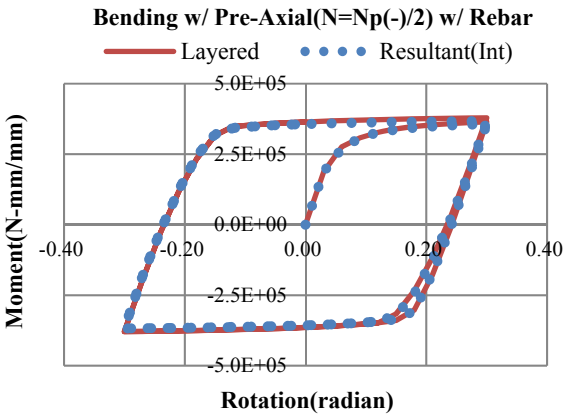

(a) Bending with pre-axial ($1/2N_p(-)$) w/o Rebar (b) Bending with pre-axial($1/2N_p(-)$) w/ Rebar

Figure 11 Bending stress resultant vs. rotation in pre-axial bending loading

5. Conclusions

A stress-resultant based elasto-plastic analysis for a concrete plate is suggested and is compared with the layered model which is commonly used in practical design. A yield function based on stress resultants is derived for the Drucker-Prager criterion which is widely used for a concrete material. Through a parametric study the basic derived yield function is modified. To get reasonable results using the derived yield function, the moment calibration parameter k and the exponent of the moment term β are introduced. The general plastic flow rule is applied to this failure function. In addition, a steel rebar model is added for the reinforcement of a concrete plate. The smeared layer method is introduced to the layered model and an integrated section method using equivalent material coefficients is suggested for the stress-resultant plate model. Several tests of unit element show that the proposed method has reasonable results under cyclic loading compared with the layered model regardless of reinforcement. In the practical example of a concrete bridge, the suggested stress-resultant model shows available accuracy and efficiency compared with the layered model.

References

[1] Crisfield, M.A. (1991) Nonlinear Finite Element Analysis of Solid and Structures. Vol. 1. *John Wiley & Sons Ltd, New York*

[2] Crisfield, M.A. (1997) Nonlinear Finite Element Analysis of Solid and Structures. Vol. 2. *John Wiley & Sons Ltd, New York*

[3] Takeda, T., Sozen, M.A., and Nielsen, N. (1970). Reinforced concrete response to simulated earthquakes. *J. Struct. Div., ASCE* 96(12), 2557-2573

[4] Hilmy, S. I., & Abel, J. F. (1985). A strain-hardening concentrated plasticity model for nonlinear dynamic analysis of steel buildings. *Proc., NUMETA85, Numerical Methods in Engineering, Theory and Applications*, *1*, 303-314.

[5] Hajjar, J. F., and Gourley, B. C. (1997). A cyclic nonlinear model for concrete-filled tubes. I: Formulation. *J. Struct. Eng.,* 123(6), 736-744.

[6] El-Tawil, S., and Deierlein, G. G. (1999). Strength and ductility of concrete encased composite columns. *J. Struct. Eng.,* 125(9), 1009-1019.

[7] El-Tawil, S., and Deierlein, G. G. (2001a). Nonlinear analysis of mixed steel-concrete moment frames. Part I: Beam-coulomb element formulation. *J. Struct. Eng.,* 127(6), 647-655.

[8] Spacone, E., & El-Tawil, S. (2004). Nonlinear analysis of steel-concrete composite structures: State of the art. *Journal of Structural Engineering*,*130*(2), 159-168.

[9] Kent, D. C., & Park, R. (1971). Flexural members with confined concrete. *Journal of the Structural Division*, *97*(7), 1969-1990.

[10] Mander, J. B., Priestly M. N. J., and Park, R. (1988). Theoretical stress-strain model for confined concrete. *J. Struct. Eng.,* 114(8), 1805-1826.

[11] Iliushin, A.A. (1956). Plastichnost', Gostekhizdat, Moscow (in Russian).

[12] Crisfield, M.A. (1981). Finite element analysis for combined material and geometric nonlinearities. In W. Wunderlich et al. (eds). Nonlinear Finite Element Analysis in Structural Mechanics, Springer-Verlag, New York, pp. 325-338.

[13] Shi, G., & Voyiadjis, G. Z. (1992). A simple non-layered finite element for the elasto-plastic analysis of shear flexible plates. *International journal for numerical methods in engineering*, 33(1), 85-99.

[14] George Z. Voyiadjis & Pawel Woelke. (2008). Elasto-Plastic and Damage Analysis of Plates and Shells. *Springer.*

[15] Koechlin, P., Andrieux, S., Millard, A., & Potapov, S. (2008). Failure criterion for reinforced concrete beams and plates subjected to membrane force, bending and shear. *European Journal of Mechanics-A/Solids*, *27*(6), 1161-1183.

[16] Bieniek and Funaro, (1976), Elasto-plastic behavior of plates and shells. Technical report DNA 3584A, *Weidlinger Associates, New York*

[17] Armstrong, P.J. and Frederick, C.O. (1966). A Mathematical Representation of the Multiaxial Bauschinger Effect. (C.E.G.B report RD/B/N 731. Berkeley Laboratories, R&D Department, California.

[18] Sam Lee, 2008, Nonlinear Dynamic Earthquake Analysis of Skyscrapers. *CTBUH8th World Congress*.

[19] Zhang, Y. X., & Bradford, M. A. (2007). Nonlinear analysis of moderately thick reinforced concrete slabs at elevated temperatures using a rectangular layered plate element with Timoshenko beam functions. *Engineering Structures*, *29*(10), 2751-2761

[20] Baskar, K., Shanmugam, N. E., & Thevendran, V. (2002). Finite-element analysis of steel-concrete composite plate girder. *Journal of Structural Engineering*, *128*(9), 1158-1168.

[21] C. Zienkiewicz and R.L. Taylor. (1989). Basic formulation and linear problems In: The Finite Element Method, Vol. 1, 4th *Edn McGraw-Hill, London*

[22] Carreira, D. J., & Chu, K. H. (1986). Stress-strain relationship for reinforced concrete in tension. In *ACI Journal Proceedings* (Vol. 83, No. 1). ACI.

[23] MIDAS NFX manual. MIDAS Information and Technology Ltd., Seoul, Korea 2011.